Journal of Photochemistry and Photobiology A: Chemistry 215 (2010) 108–117

Contents lists available at ScienceDirect

Journal of Photochemistry and Photobiology A: Chemistry

journal homepage: www.elsevier.com/locate/jphotochem

pH dependence of the absorption and emission behaviour of lumiflavin in aqueous solution

A. Tyagi, A. Penzkofer*

Fakultät für Physik, Universität Regensburg, Universitätsstrasse 31, D-93053 Regensburg, Germany

ARTICLE INFO

Article history:
Received 24 May 2010
Received in revised form 5 July 2010
Accepted 4 August 2010
Available online 11 August 2010

Keywords:
Lumiflavin
pH dependent absorption
pH dependent fluorescence
Fluorescence quantum yields
Fluorescence lifetimes
Ground-state ionization equilibrium constants
Relaxation dynamics

ABSTRACT

The spectroscopic behaviour of lumiflavin (7,8,10-trimethyl-isoalloxazine, oxidized form LF_{ox}) in aqueous solutions of pH range −1.08 to 14.6 is studied. Absorption spectra, fluorescence quantum distributions, quantum yields and lifetimes are determined. The ionization stage of ground-state LF_{ox} changes from cationic ($LF_{ox}H_2^+$) at low pH ($pK_c \approx 0.38$) via neutral ($LF_{ox}H$) to anionic (LF_{ox}^-) at high pH ($pK_a \approx 10.8$). The cationic, neutral, and anionic forms are identified by their different absorption spectra. $LF_{ox}H$ in neutral aqueous solution is reasonably fluorescent (fluorescence quantum yield $\phi_F \approx 0.29$, fluorescence lifetime $\tau_F \approx 5.2$ ns), while LF_{ox}^- is weakly fluorescent ($\phi_F \approx 0.0042$, $\tau_F \approx 90$ ps), and $LF_{ox}H_2^+$ is nearly non-fluorescent ($\phi_F \approx 3.6 \times 10^{-5}$, $\tau_F \approx 0.4$ ps).

A theory of the pH dependent equilibration of cationic, neutral and anionic molecules in the ground state and their dynamics in the excited state is developed. For lumiflavin in aqueous solution in the excited state no equilibrium distributions are reached between the cationic, neutral, and anionic forms. Some neutral excited lumiflavin transforms to the cationic ground-state form at low pH by intermolecular photo-induced proton transfer from H_3O^+ to $LF_{ox}H^*$. At high pH no photo-induced intermolecular proton transfer takes place.

1. Introduction

Lumiflavin (7,8,10-trimethyl-isoalloxazine, LF) is the fundamental molecule of the huge class of flavins with the most famous members riboflavin (RF), flavin mononucleotide (FMN), and flavin adenine dinucleotide (FAD) [1,2]. Lumiflavin is the dominant photoproduct of RF, FMN, and FAD in alkaline solution (pH > 9) [2–6]. It is obtained by photolysis of riboflavin in 1 M NaOH [4,7]. Ways of synthesis of lumiflavin are described in [8–10]. Lumiflavin is a photo-sensitizer of organic and biological molecules by radical formation (type I photosensitization) and singlet oxygen generation (type II photosensitization) [11–17].

The photo-physical behaviour of lumiflavin is described in [1,3,4,12,18–25]. Absorption spectroscopy [3,4,7,15,18,20,25], fluorescence spectroscopy [12,19,20], and triplet spectroscopy [12,19–22] were carried out for lumiflavin characterization. The pH dependence of fluorescence was studied [26,27]. Ionization equilibria between cationic, neutral and anionic forms in the ground state [28,29], singlet excited state [28], and triplet excited state [30] were determined. The photo-stability of lumiflavin in aqueous solutions [3,4,25], organic solvents [3–5], and in biological matter [11–15] was investigated. In alkaline solution at elevated temperatures lumiflavin was found to be thermally unstable by hydrolysis reaction [31,32]. Quantum chemical calculations on electronic structure, molecular properties, and spectroscopic parameters of lumiflavin were carried out [23,33–40]. Thereby lumiflavin served as prototype of flavins.

Despite the long period of lumiflavin investigation no detailed absolute absorption cross-section spectra, no absolute intrinsic fluorescence quantum distributions and quantum yields as well as no fluorescence decay curves over the experimentally accessible pH range from −1.08 (37% HCl) to 14.6 (4 M NaOH) are available. The mechanisms of fluorescence quenching of lumiflavin in neutral ($LF_{ox}H$), cationic ($LF_{ox}H_2^+$), and anionic form (LF_{ox}^-) have not been worked out. The difference in the constants of ground-state equilibrium, pK_c, and singlet excited equilibrium, pK_c^*, between cationic and neutral lumiflavin, and the equality of the constants of ground-state equilibrium, pK_a, and singlet excited equilibrium, pK_a^*, between neutral and anionic lumiflavin has not yet been satisfactorily explained.

In this paper we work on these topics. The behaviour of the absolute absorption cross-section spectra, the absolute fluorescence quantum distributions, the absolute fluorescence quantum yields, and the fluorescence lifetimes of lumiflavin in aqueous solution are studied over the range from pH −1.08 to pH 14.6. The absorption and emission dependences are inter-

* Corresponding author at: Universität Regensburg, Fakultät für Physik, Universitätsstrasse 31, D-93053 Regensburg, Germany. Tel.: +49 941 943 2107; fax: +49 941 943 2754.
E-mail address: alfons.penzkofer@physik.uni-regensburg.de (A. Penzkofer).

1010-6030/$ – see front matter © 2010 Elsevier B.V. All rights reserved.
doi:10.1016/j.jphotochem.2010.08.007

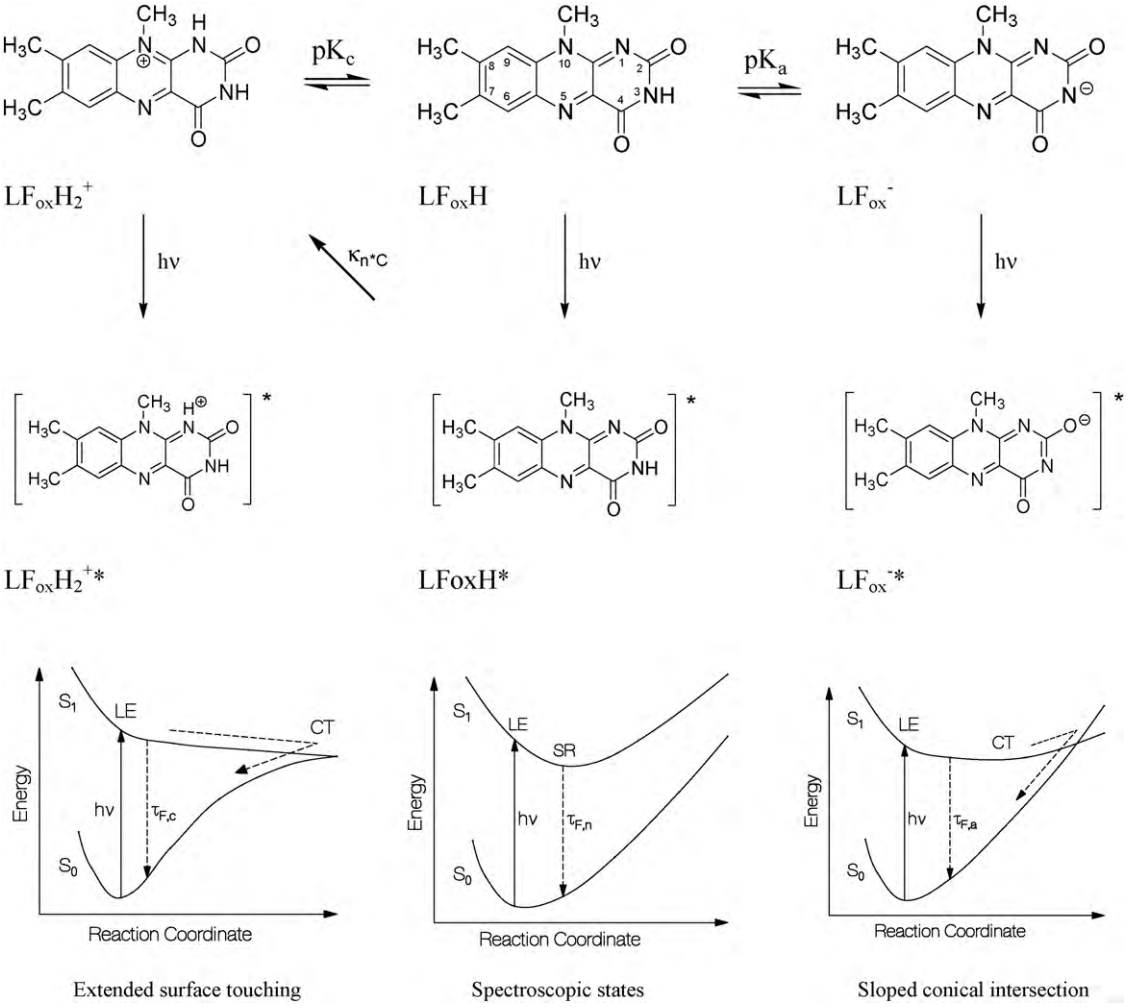

Fig. 1. Top row: structural formulae of cationic, neutral, and anionic lumiflavin in the oxidized (flavoquinone) redox state (taken from [2]) with thermal equilibrium paths (pK_c and pK_a). Middle row: possible structural formulae of cationic, neutral, and anionic lumiflavin in the excited state. Bottom row: illustrative potential energy curves for ground state and first excited state of cationic, neutral, and anionic lumiflavin. Transitions are indicated.

preted in terms of photo-physical and photochemical interactions (photo-physical fluorescence quenching of $LF_{ox}H$ at neutral pH, intra-molecular charge transfer for $LF_{ox}H_2^+$ and LF_{ox}^-). The pK values of cationic–neutral equilibrium (pK_c) and neutral–anionic equilibrium (pK_a) in the ground state are extracted from the absorption dependences. In the excited state no ionization state equilibria are reached within the short fluorescence lifetimes. Therefore no equilibration constants, pK_c^* and pK_a^*, are accessible. Instead, pH values pK_{Fc}^* and pK_{Fa}^* of mid-point fluorescence efficiency between cationic and neutral species as well as between neutral and anionic species will be determined by pH dependent fluorescence quantum yield measurements. A theory of the pH dependent equilibration of cationic, neutral and anionic molecules in the ground state and their dynamics in the excited state will be developed. The inequality $pK_c < pK_{Fc}^*$ will be explained by intermolecular proton transfer deactivation of neutral excited lumiflavin $LF_{ox}H^*$ at low pH ($LF_{ox}H^* + H^+ \rightarrow LF_{ox}H_2^+$).

The structural formulae of lumiflavin in the flavoquinone (oxidized) redox state in neutral form ($LF_{ox}H$), in cationic form ($LF_{ox}H_2^+$), and in anionic form (LF_{ox}^-) are shown in the top row of Fig. 1. The flavosemiquinone (semi-reduced) redox state ($LFH_2^\bullet$) and the flavohydroquinone (fully reduced) redox state ($LF_{red}H_3$) of lumiflavin are not present under our experimental conditions (aerobic solutions, no added reducing agents) [1,2,41]. Therefore the complex photo-dynamics of semi-reduced and fully reduced flavins in their neutral, cationic, and anionic form [42–44] is not addressed here.

2. Experimental

Lumiflavin (LF) was purchased from Sigma–Aldrich and used as delivered. The dye was dissolved in aqueous solutions of different pH. At lowest pH (−1.08) LF was dissolved in concentrated hydrochloric acid (37 wt.% HCl). In the range of pH −0.3 (2 M HCl) to pH 3 (10^{-3} M HCl) differently concentrated aqueous HCl solutions, and in the range of pH 11 (10^{-3} M NaOH) to 14.6 (4 M NaOH) differently concentrated NaOH solutions were used. A citric acid/NaOH/NaCl buffer (Fixanal from Aldrich) was used for pH 4. For pH 6, pH 8, and pH 10 self-prepared 10 mM sodium phosphate buffers with 10 mM NaCl were used. All measurements were carried out at room temperature under aerobic conditions.

The absorption spectra were measured with a commercial spectrophotometer (Cary 50 from Varian). The fluorescence emission spectra were recorded with a commercial fluorimeter (Cary Eclipse from Varian) under magic angle conditions. The spectra were corrected for the spectral sensitivities. For absolute intrinsic fluorescence quantum distribution and quantum yield calibration the dyes riboflavin in water ($\phi_F = 0.26$ [45]) and POPOP (1,4-di(5-phenyloxazolyl)benzene) in ethanol ($\phi_F = 0.85$ [46]) were used as reference standards.

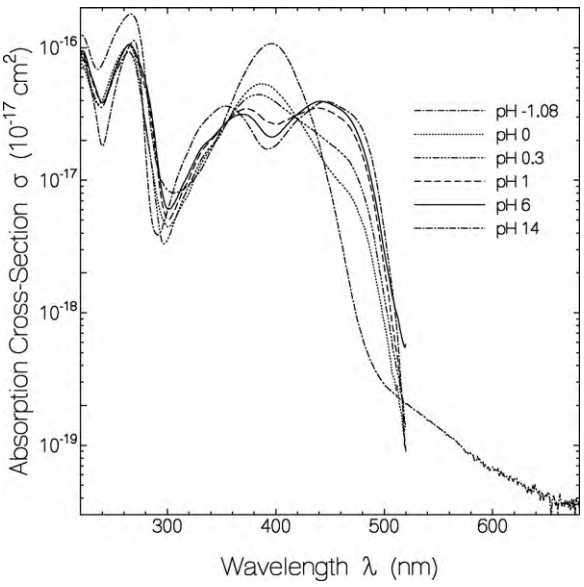

Fig. 2. Absorption cross-section spectra of lumiflavin in aqueous solution at different pH values.

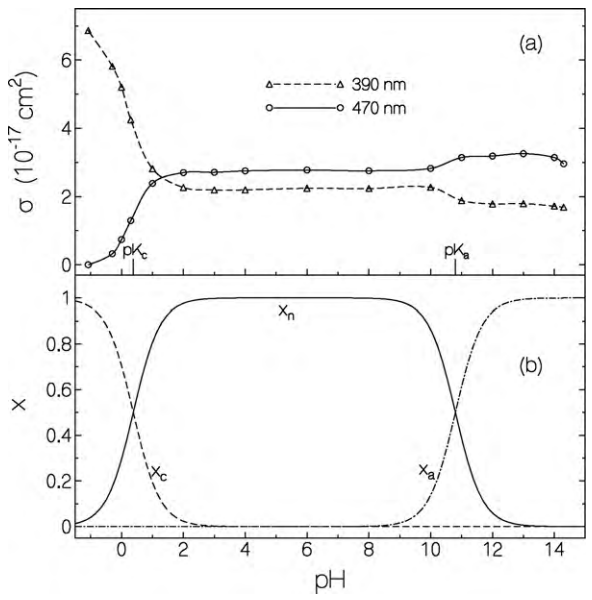

Fig. 3. (a) Absorption cross-sections of lumiflavin in aqueous solution versus pH for two selected wavelengths, 390 nm and 470 nm. (b) Mole fractions of cationic form, x_c, neutral form, x_n, and anionic form, x_a, of lumiflavin in aqueous solution versus pH (Eqs. (2d), (4d), and $x_n = 1 - x_c - x_a$).

Time-resolved fluorescence traces were measured by using a mode-locked titanium–sapphire laser oscillator amplifier system (Hurricane from Spectra Physics) and an ultrafast streak-camera (type C1587 temporal disperser with M1952 high-speed streak unit from Hamamatsu) [47]. At 400 nm second harmonic pulses, and at 456 nm Raman-shifted second harmonic pulses (Raman medium ethanol) [48] were used for excitation.

3. Results

Absorption cross-section spectra, $\sigma(\lambda)$, of the studied lumiflavin samples are shown in Fig. 2. They were calculated from measured transmission spectra ($\sigma = -\ln(T)/(\ell N_0)$), T: transmission, ℓ: sample length, N_0: molecule number density). The lumiflavin concentration was around 1.7×10^{-5} mol dm^{-3}. Molar decadic absorption coefficient spectra, $\varepsilon(\lambda)$, are related to the absorption cross-section spectra by $\varepsilon(\lambda) = \sigma(\lambda) N_A/[1000 \ln(10)]$, where N_A is the Avogadro constant. The maximum S_0–S_1 absorption cross-sections, $\sigma_{a,max}$, the corresponding wavelength positions, $\lambda_{a,max}$, and the spectral S_0–S_1 absorption half-widths (FWHM), $\Delta\tilde{\nu}_a$, of the samples investigated here are collected in Table 1.

The absorption spectra are unchanged in the range from pH 2 to pH 10 where the neutral form of LF_{ox} is dominant. The presented spectrum for pH 6 is equal to the spectrum of the neutral form of lumiflavin ($LF_{ox}H$). In the range from pH 11 to pH 14.6 the absorption spectra have approximately the same shape and magnitude as the curve shown for pH 14. This spectrum is equal to the spectrum of the anionic form of lumiflavin (LF_{ox}^-). Below pH 2 the shape of the absorption spectra changes strongly from a double-peaked spectrum belonging to $LF_{ox}H$ (maxima at 441 nm and 370 nm) to a single peaked spectrum (maximum at 394 nm) of $LF_{ox}H_2^+$. The spectrum at pH −1.08 gives the absorption coefficient spectrum of cationic lumiflavin with approximately 3.4% neutral lumiflavin contribution (see below) and a long-wavelength absorption tail likely from small fractions of constitutional isomers and aggregates of cationic lumiflavin, and of bi-cationic lumiflavin [49] (has absorption shoulder around 520 nm).

In Fig. 3a the dependence of the absorption cross-sections σ(390 nm) and σ(470 nm) versus pH are plotted. The mid-point of absorption change at pH 0.38 at the low pH side gives the minus decadic logarithm of the H^+ concentration, called pK_c, where the concentration $[LF_{ox}H_2^+]$ of cationic lumiflavin and the concentration $[LF_{ox}H]$ of neutral lumiflavin are equal [45] (i.e. $pK_c = -\log([H^+]_c/(1\,\text{mol dm}^{-3})) = 0.38$, and $[H^+]_c = 0.42$ mol dm^{-3}). The mid-point of absorption change at the high pH side occurs at about pH 10.8. It gives the minus decadic logarithm of the H^+ concentration, called pK_a, where the concentrations $[LF_{ox}H]$ and $[LF_{ox}^-]$ are equal [45] (i.e. $pK_a = -\log([H^+]_a/(1\,\text{mol dm}^{-3})) = 10.8$, and $[H^+]_a = 1.8 \times 10^{-11}$ mol dm^{-3}).

The fluorescence quantum distributions, $E_F(\lambda)$, of lumiflavin aqueous solutions at several pH values are shown in Fig. 4a for fluorescence excitation wavelength $\lambda_{exc} = 450$ nm and in Fig. 4b for $\lambda_{exc} = 350$ nm. Fluorescence quantum distributions of lumiflavin at pH −1.08 for different excitation wavelengths are depicted in Fig. 4c. In the case of fluorescence excitation at $\lambda_{exc} = 450$ nm (Fig. 4a) the fluorescence emission belongs dominantly to $LF_{ox}H$ in the range $-0.3 \le$ pH ≤ 12, and to LF_{ox}^- in the range pH > 12. In the case of fluorescence excitation at $\lambda_{exc} = 350$ nm at low pH (Fig. 4b) the fluorescence in the short wavelength part (<500 nm) belongs to $LF_{ox}H_2^+$, and above 500 nm both $LF_{ox}H$ and $LF_{ox}H_2^+$ contribute to the fluorescence spectrum.

The determined fluorescence quantum yields, $\phi_F = \int E_F(\lambda) d\lambda$, versus pH are displayed in Fig. 5 for $\lambda_{exc} = 350$ nm (triangles) and $\lambda_{exc} = 450$ nm (circles). In the range 3 < pH < 10 the fluorescence quantum yield has a high plateau of $\phi_F \approx 0.29$. At lower and higher pH the fluorescence quantum yield drops down. At the high pH side the pH position of fluorescence decrease coincides with the change from the ground state neutral form to the ground-state anionic form (pK_a = 10.8, see Fig. 3). A minimum of fluorescence emission is reached at pH ≈ 14 with $\phi_F \approx 0.0042$. The fluorescence efficiency rises slightly at higher pH because of fluorescence contributions from thermally degraded species [31,32] (degradations studies will be reported elsewhere). At the low pH side the fluorescence quantum yield decreases already at higher pH than the ground-state cationic–neutral equilibrium (pK_c = 0.38, see Fig. 3).

The determined fluorescence quantum yields for $\lambda_{exc} = 450$ nm are listed in Table 1. The relative error of the determined fluorescence quantum yields is between 5% and 10%. The wavelength positions, $\lambda_{F,max}$, of peak fluorescence emission, the spectral half-widths (FWHM) of the emission spectra, $\Delta\tilde{\nu}_F$, and the flu-

Table 1
Spectroscopic parameters of lumiflavin in aqueous solutions of different pH.

pH	$\phi_F(\lambda_{exc}=450nm)$	$\lambda_{a,max}$ (nm)	$\sigma_{a,max}$ (cm^2)	$\Delta\tilde{\nu}_a$ (cm^{-1})	$\lambda_{F,max}$ (nm)	$\Delta\tilde{\nu}_F$ (cm^{-1})	$\delta\tilde{\nu}_{St}$ (cm^{-1})
−1.08	$(3.2\pm0.3)\times10^{-4}$	394	7.0×10^{-17}	3710	≈435	≈4000	≈2400
−0.3	0.002 ± 0.0004	389	5.9×10^{-17}	4100	460	5500	3970
0	0.0042 ± 0.0004	386	5.3×10^{-17}	4570	522	5680	6750
0.3	0.0093 ± 0.001	384	4.4×10^{-17}	5840	530	3370	7170
1	0.0415 ± 0.004	439	3.0×10^{-17}	4390	532	3089	3982
2	0.18 ± 0.02	441	3.8×10^{-17}	4430	532	3041	3879
3	0.279 ± 0.01	441	3.8×10^{-17}	4430	531	3065	3843
4	0.29 ± 0.01	441	3.9×10^{-17}	4430	531	3065	3843
6	0.29 ± 0.01	441	3.9×10^{-17}	4430	529	3065	3772
8	0.29 ± 0.01	441	3.9×10^{-17}	4430	528	3065	3736
10	0.28 ± 0.01	441	4.0×10^{-17}	4430	528	3030	3736
11	0.105 ± 0.01	442	4.0×10^{-17}	4220	530	3100	3757
12	0.021 ± 0.003	445	4.0×10^{-17}	4230	529	3141	3568
13	0.0055 ± 0.001	446	4.0×10^{-17}	4140	528	3229	3482
14	0.0042 ± 0.0008	446	3.9×10^{-17}	4104	529	3248	3518
14.3	0.0051 ± 0.0008	446	3.7×10^{-17}	4215	528	3214	3482
14.6	0.0066 ± 0.0008	446	3.3×10^{-17}	4860	530	3188	3550

Abbreviations: ϕ_F: fluorescence quantum yield; $\lambda_{a,max}$: wavelength of S_0–S_1 absorption maximum; $\sigma_{a,max}$: peak S_0–S_1 absorption cross-section; $\Delta\tilde{\nu}_a$: full spectral half-width of first absorption band; $\lambda_{F,max}$: wavelength position of maximum fluorescence emission; $\Delta\tilde{\nu}_F$: full spectral half-width fluorescence band; $\delta\tilde{\nu}_{St}$: fluorescence Stokes shift ($\delta\tilde{\nu}_{St}=\lambda_{a,max}^{-1}-\lambda_{F,max}^{-1}$).

orescence Stokes shift, $\delta\tilde{\nu}_{St}=(\lambda_{a,max}^{-1}-\lambda_{F,max}^{-1})$, are included in Table 1.

For lumiflavin in 37 wt.% HCl (pH −1.08) the fluorescence behaviour is rather complex as is shown in Fig. 4c. The fluorescence quantum distributions and the fluorescence quantum yields depend on the fluorescence excitation wavelength, λ_{exc}. At this low pH lumflavin dominantly consists of the single-cationic form, $LF_{ox}H_2^+$, about 3.4% of the neutral form (see below), $LF_{ox}H$, a fraction of the bi-cationic form, $LF_{ox}H_3^{2+}$ [49], constitutional isomers and aggregates of $LF_{ox}H_2^+$. Fluorescence quantum distributions for a few different excitation wavelengths are shown in the top part of Fig. 4c: In the case of excitation at 260 nm the fluorescence spectrum is likely dominated by impurity emission (wavelength region 300–480 nm, fluorescence quantum yield $\phi_F\approx4.9\times10^{-5}$) and S_1–S_0 emission from the first $LF_{ox}H_2^+$ absorption band (region > 480 nm, $\phi_F\approx3.6\times10^{-5}$). Excitation at 300 nm (weak absorption of $LF_{ox}H_2^+$) indicates impurity emission (wavelength 320–500 nm, $\phi_F\approx3.4\times10^{-4}$) and likely $LF_{ox}H_3^{2+}$ emission (wavelength > 500 nm $\phi_F\approx3.6\times10^{-4}$). Excitation at 380 nm (dominant absorption band of $LF_{ox}H_2^+$) gives dominantly S_1–S_0 emission from $LF_{ox}H_2^+$ (460–680 nm, efficiency 3.6×10^{-5}) and S_1–S_0 emission likely from an $LF_{ox}H_2^+$ structural isomer or aggregate (>680 nm, efficiency 1.6×10^{-5}; low efficiency because of low absorption contribution at 380 nm). In the case of excitation at 460 nm the fluorescence is thought to come from $LF_{ox}H$ and $LF_{ox}H_3^{2+}$ (peak at 550 nm, efficiency 2.4×10^{-4}) and from a structural $LF_{ox}H_2^+$ isomer or aggregate (peak at 720 nm, efficiency 3.9×10^{-4}). In the case of excitation at 500 nm the emission comes likely from $LF_{ox}H_3^{2+}$ with efficiency of 0.0017 (520–700 nm) and from an $LF_{ox}H_2^+$ isomer with efficiency of 0.0031 (λ_F > 700 nm). For λ_{exc} = 500 nm the fluorescence efficiency is higher than for λ_{exc} = 460 nm since at 460 nm most light is absorbed by the nearly non-fluorescent $LF_{ox}H_2^+$ (quantum yields are defined here as emitted photons from considered transition to total number of absorbed photons).

The dependence of the total fluorescence quantum yield, ϕ_F, of lumiflavin in 37 wt.% HCl on the excitation wavelength, λ_{exc}, is depicted in lower part of Fig. 4c together with the absorption cross-section spectrum of lumiflavin in 37 wt.% HCl.

Normalized fluorescence signal decay curves, $S_F(t)/S_{F,max}$, of lumiflavin in aqueous solution at several pH values are presented in Fig. 6a–c. In the range pH < 10 the fluorescence after picosecond pulse excitation decays single-exponentially, i.e. $S_F(t)=S_{F,max}\exp(-t/\tau_F)$. In the range 3 < pH < 10 the fluorescence decay is approximately unchanged with a fluorescence lifetime of $\tau_F\approx5.2$ ns. Below pH 3 the fluorescence lifetime τ_F decreases because of additional $LF_{ox}H^*$ deactivation by intermolecular protonation according to $LF_{ox}H^*+H^+\rightarrow LF_{ox}H_2^+$ (see below). For lumiflavin in 37 wt.% HCl (pH −1.08) and λ_{exc} = 400 nm the fluorescence decay could not be resolved experimentally. An upper limit of 2.3 ps was obtained. From the measured fluorescence quantum yield of $\phi_F(\lambda_{exc}=400\,nm)\approx3.6\times10^{-5}$ and the estimated radiative lifetime of $\tau_{rad}\approx11.6$ ns a fluores-

Table 2
Reported pK values for flavins.

Flavin	pK_c	pK_{Fc}*	pK_a	pK_{Fa}*	References
Lumiflavin	−0.2		9.8		[29]
	0.0	1.7			[28]
		1.7		10.1	[27]
		2.3		9.8	[26]
	0.38	1.8	10.8	10.8	This work
Riboflavin	0.12		9.95		[16]
	−0.2		9.8		[29]
			9.93[a]		[61]
	−0.1	1.7			[28]
		1.6		10.3	[27]
		2.3		9.8	[26]
	0.4	2.3	9.75	9.75	[45]
FMN	0.05		10.32		[16]

[a] Determined with electrochemical method. pK values were determined by absorption spectroscopy. pK_F* values were determined by fluorescence spectroscopy.

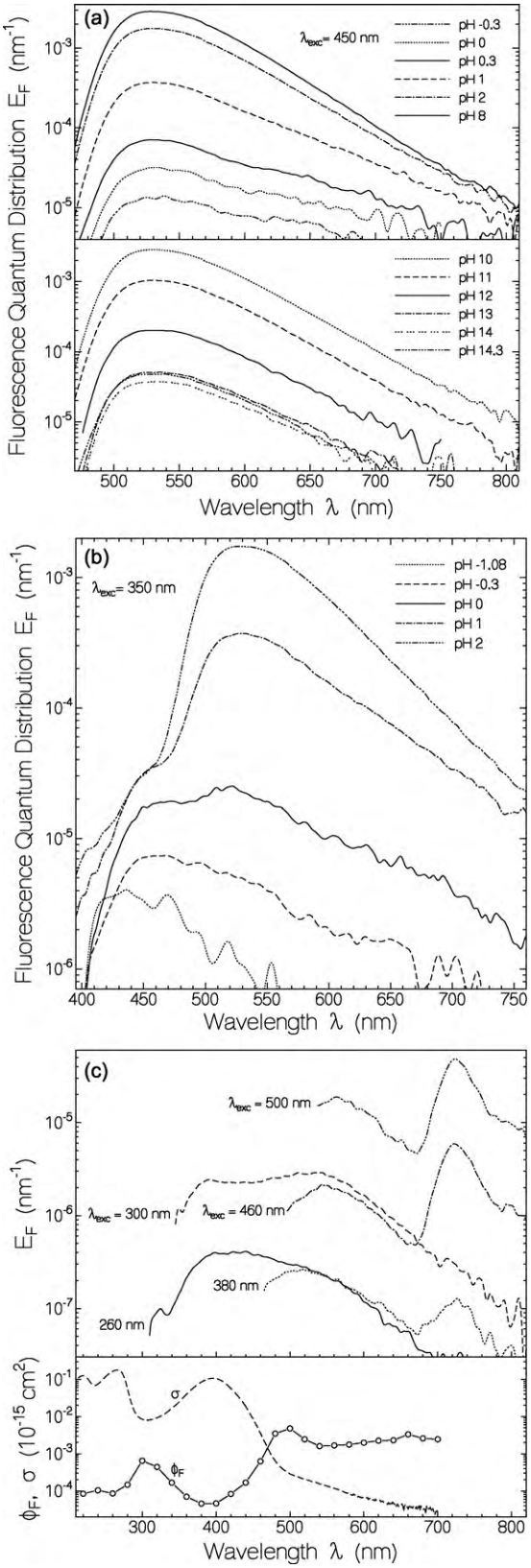

Fig. 4. Fluorescence quantum distributions, $E_F(\lambda)$, of lumiflavin in aqueous solution at different pH values. (a) Fluorescence excitation wavelength, λ_{exc} = 450 nm. (b) Fluorescence excitation wavelength, λ_{exc} = 350 nm. (c) Fluorescence behaviour of lumiflavin in 37 wt.% HCl (pH −1.08). Top part: $E_F(\lambda)$ for some excitation wavelengths. Bottom part: fluorescence quantum yield, ϕ_F, and absorption cross-section, σ, versus excitation wavelength.

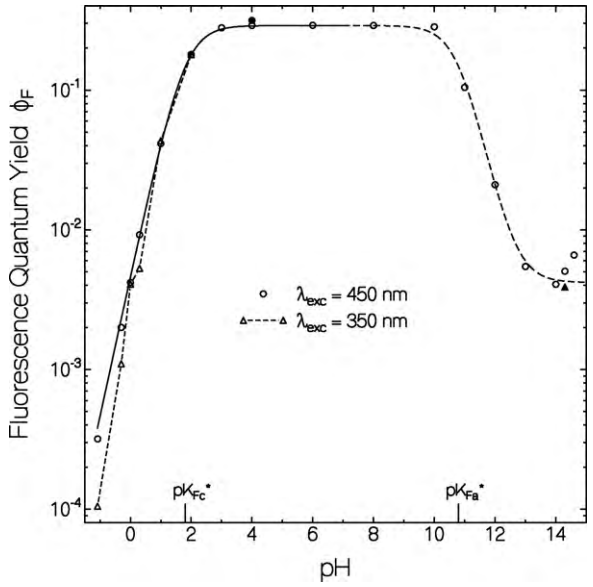

Fig. 5. Fluorescence quantum yields of lumiflavin in aqueous solution versus pH. Buffer composition is given in the experimental part. Exceptions are filled circle (1×10^{-4} M HCl, λ_{exc} = 450 nm) and filled triangle (2 M KOH, λ_{exc} = 450 nm). Solid curve is calculated by use of Eq. (9), with $\phi_{F,0,n} = 0.29$, $\tau_{F,0,n} = 5.2$ ns, and $\kappa_{n^*c} = 1.2 \times 10^{10}$ mol^{-1} s^{-1}. Dashed curve is calculated by use of $\phi_F(\mathrm{pH}) = x_n(\mathrm{pH})\phi_{F,0,n} + x_a(\mathrm{pH})\phi_{F,a}$ with $\phi_{F,0,n} = 0.29$ and $\phi_{F,a} = 0.0042$, $x_a = N_a/N_0$ (Eq. (4d)), and $x_n = 1 - x_a$.

cence lifetime of $\tau_F(400\,\mathrm{nm}) = \phi_F(400\,\mathrm{nm})\tau_{rad} \approx 0.4$ ps is estimated. It gives the S_1–S_0 fluorescence lifetime of cationic lumiflavin, i.e. $\tau_{F,c} \approx 0.4$ ps. The curves for pH 11 and pH 12 (Fig. 6c) exhibit bi-exponential fluorescence decay according to $S_F(t)/S_{F,max} = x_{F,n}\exp(-t/\tau_{F,n}) + x_{F,a}\exp(-t/\tau_{F,a})$ with $x_{F,a} = 1 - x_{F,n}$. The slow fluorescence component with fraction $x_{F,n}$, belongs to neutral lumiflavin emission and the short fluorescence component with fraction $x_{F,a}$, belongs to anionic lumiflavin emission.

The extracted fluorescence lifetimes from the fluorescence decay measurements (Fig. 6), τ_F (circles), $\tau_{F,n}$ (diamonds), and $\tau_{F,a}$ (triangles), versus pH are displayed in Fig. 7a. The fractions, $x_{F,n}$ and $x_{F,a}$, of the slow and fast fluorescence components versus pH are shown in Fig. 7b (see below).

The filled symbols in Fig. 7a (fluorescence lifetime) and in Fig. 5 (fluorescence quantum yield) indicate some dependence of the fluorescence behaviour (fluorescence quenching) on the buffer composition: The filled circles at pH 4 belong to 10^{-4} M HCl solution, and at pH 14.3 the filled triangles belong to 2 M KOH solution.

4. Discussion

4.1. Absorption cross-sections and radiative lifetimes

The absorption cross-section spectra of $LF_{ox}H_2^+$ (σ_c), of $LF_{ox}H$ (σ_n), and of LF_{ox}^- (σ_a) are approximately given by $\sigma_n(\lambda) = \sigma(\lambda, \mathrm{pH}\ 6)$, $\sigma_a(\lambda) = \sigma(\lambda, \mathrm{pH}\ 14)$, $\sigma_c(\lambda) = [\sigma(\lambda, \mathrm{pH}\ -1.08) - x_n\sigma_n(\lambda)]/(1 - x_n)$ with $x_n = 0.034$ (Fig. 2, see below). The S_0–S_1 absorption strengths $\bar{\sigma} = \int_{S_0-S_1}[\sigma(\lambda)/\lambda]d\lambda$ of the three ionic forms are $\bar{\sigma}_c \approx 6.6 \times 10^{-17}$ cm^2 (used upper wavelength limit of S_0–S_1 absorption band λ_u = 398 nm, S_0–S_1 and S_0–S_2 transitions are thought to be merged in broad absorption band), $\bar{\sigma}_n = 6.45 \times 10^{-18}$ cm^2 (λ_u = 395 nm), and $\bar{\sigma}_a = 6.41 \times 10^{-18}$ cm^2 (λ_u = 395 nm).

The radiative lifetimes of the different ionic forms are obtained by application of the Strickler–Berg formula [50–52]

$$\tau_{rad} = \frac{n_A\bar{\lambda}_F^3}{8\pi c_0 n_F^3\bar{\sigma}}, \quad (1)$$

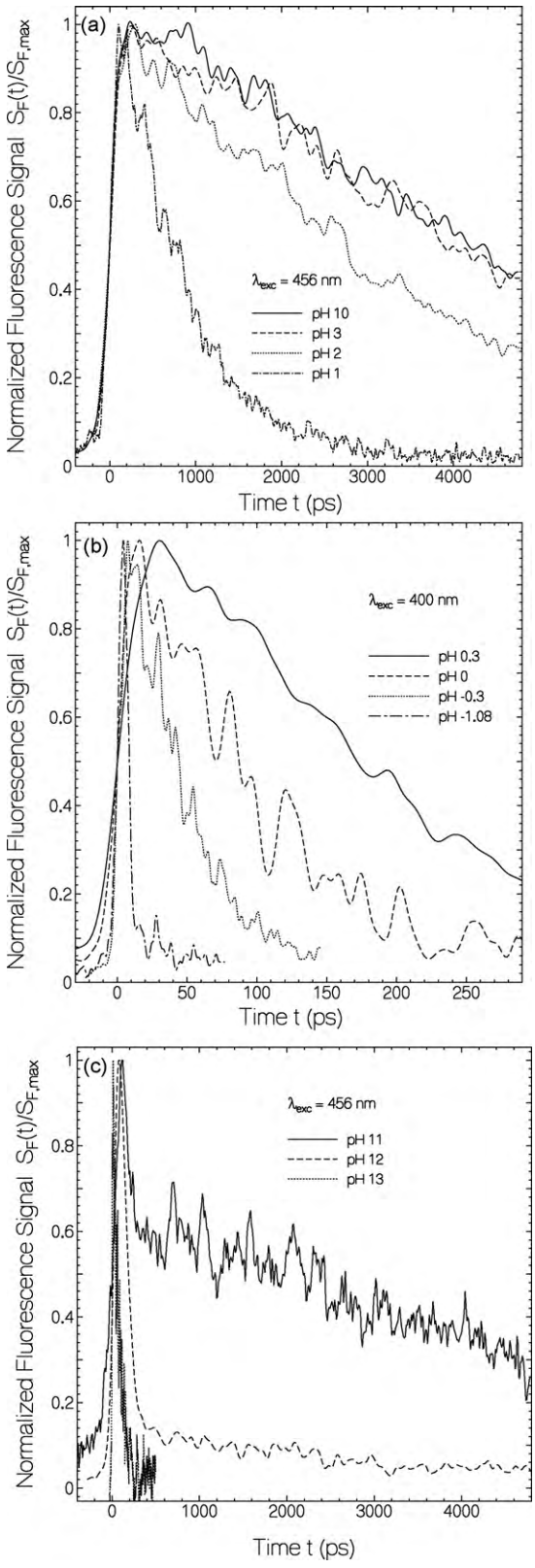

Fig. 6. Normalized temporal fluorescence signal traces, $S_F(t)/S_{F,max}$, of lumiflavin in aqueous solution of different pH. The pH values are given in the figure legends. (a and c) Fluorescence excitation wavelength λ_{exc} = 456 nm. Excitation pulse duration Δt_{exc} = 4 ps. Fluorescence detection wavelength region $\lambda_{F,det}$ > 500 nm. (b) λ_{exc} = 400 nm, Δt_{exc} = 2.5 ps, and $\lambda_{F,det}$ > 500 nm.

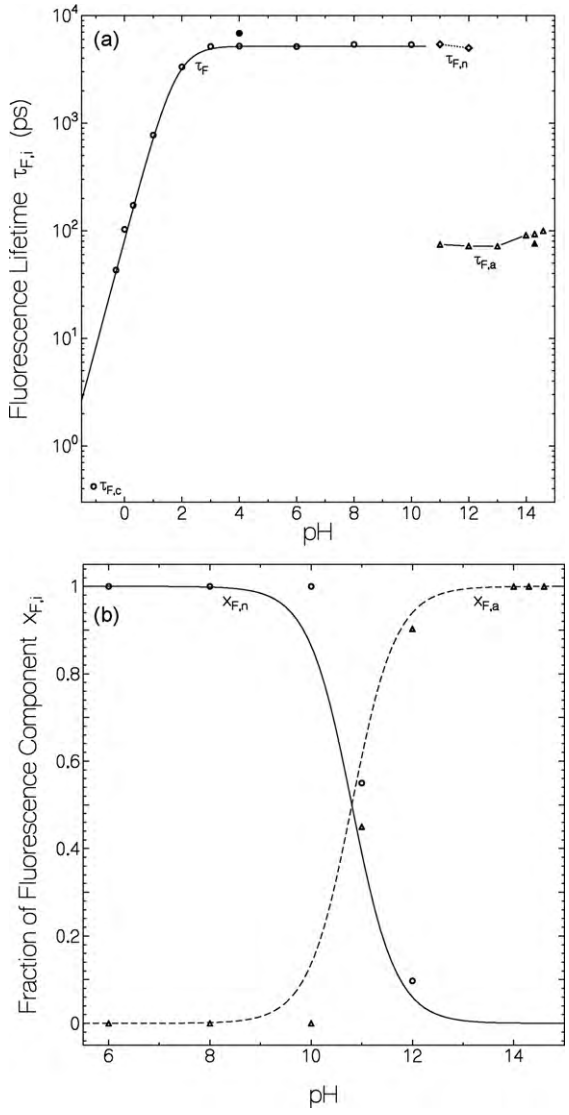

Fig. 7. (a) pH dependence of fluorescence lifetimes of lumiflavin in aqueous solution. Buffer composition is given in the experimental part. Exceptions are filled circle (1×10^{-4} M HCl) and filled triangle (2 M KOH). Values are extracted from fluorescence traces depicted in Fig. 6. τ_F is single-exponential time constant. $\tau_{F,c}$, $\tau_{F,n}$, and $\tau_{F,a}$, are fluorescence lifetimes of cationic, neutral and anionic forms. Solid curve is calculated by use of Eq. (8) with $\tau_{F,0,n}$ = 5.2 ns, and κ_{n^*c} = 1.2×10^{10} mol^{-1} s^{-1}. (b) Fractions of $LF_{ox}H$ and LF_{ox}^- initial fluorescence signal heights, $x_{F,n}$ and $x_{F,a}$, versus pH. Curves are calculated by use of Eqs. (12a) and (12b) with $\tau_{rad,n}$ = 20.7 ns, $\tau_{rad,a}$ = 21.6 ns, $\sigma_n(\lambda_{exc}$ = 456 nm) = 3.57×10^{-17} cm^2, and $\sigma_a(\lambda_{exc}$ = 456 nm) = 3.69×10^{-17} cm^2.

where n_A and n_F are the average refractive indices of the solution in the S_0–S_1 absorption and emission region, respectively ($n_A \approx n_F \approx 1.33$ in aqueous solution), c_0 is the speed of light in vacuum, and $\bar{\lambda}_F = \left[\int E_F(\lambda)\lambda^3 d\lambda / \int E_F(\lambda) d\lambda\right]^{1/3}$ is the mean fluorescence wavelength ($\bar{\lambda}_F = 469$ nm for $LF_{ox}H_2^+$, $\bar{\lambda}_F = 562$ nm for $LF_{ox}H$, and $\bar{\lambda}_F = 569$ nm for LF_{ox}^-). The calculated radiative lifetimes are $\tau_{rad}(LF_{ox}H_2^+) \approx 11.6$ ns, $\tau_{rad}(LF_{ox}H) = 20.7$ ns, and $\tau_{rad}(LF_{ox}^-) = 21.6$ ns.

$LF_{ox}H$ and LF_{ox}^- have the typical isoalloxazine structure (N5=C4a–C10a=N1, see top row of Fig. 1) with the typical isoalloxazine absorption spectrum seen in Fig. 2 (first absorption band maximum is at around 450 nm). $LF_{ox}H_2^+$ has a typical alloxazine structure (N5=C4a–C10a=N10, see Fig. 1) with a more alloxazine (lumichrome) like absorption spectrum (first absorption band of lumichrome at around 390 nm) [1,2].

4.2. Ground-state ionization distribution

The LF_{ox} ground state composition interplay of $LF_{ox}H_2^+$ and $LF_{ox}H$, in aqueous solution for pH ≤ 7 is given by reaction (R1):

$$LF_{ox}H_2^+ + H_2O \underset{\kappa_{nc}[H^+]}{\overset{k_{cn}}{\rightleftharpoons}} LF_{ox}H + H_3O^+. \quad (R1)$$

The κ parameter is a bi-molecular rate constant (dimension $s^{-1}\,M^{-1}$), and the k parameter is a uni-molecular reaction rate constant (dimension s^{-1}, $k = \kappa[H_2O]$). The steady-state ground-state thermodynamic equilibrium between $LF_{ox}H$ and $LF_{ox}H_2^+$ is given by

$$\frac{dN_n}{dt} = k_{cn}N_c - \kappa_{nc}[H^+]N_n = 0, \quad (2a)$$

$$\frac{dN_c}{dt} = -k_{cn}N_c + \kappa_{nc}[H^+]N_n = 0, \quad (2b)$$

with

$$N_n + N_c = N_0, \quad (2c)$$

leading to

$$N_c = \frac{N_0}{1 + K_c/[H^+]} = \frac{N_0}{1 + 10^{-pK_c}/10^{-pH}}, \quad (2d)$$

with the cationic–neutral equilibrium constant $K_c = k_{cn}/\kappa_{nc} = [H^+]N_n/N_c$ (Eq. (2a)) and $pK_c = -\log(K_c/1\,M)$. H^+ and $[H^+]$ are short writings of H_3O^+ and $[H_3O^+]$. N_c and N_n are the number densities of cationic and neutral lumiflavin, respectively. N_0 is the total number density of lumiflavin. $[H^+] = 10^{-pH}\,mol\,dm^{-3}$ is the concentration of H_3O^+.

Solving Eq. (2a) for $[H^+]$ gives $[H^+] = (k_{cn}/\kappa_{nc})N_c/N_n = K_cN_c/N_n$ or

$$pH = -\log([H^+]) = -\log(K_c) - \log\left(\frac{N_c}{N_n}\right) = pK_c - \log\left(\frac{N_c}{N_n}\right), \quad (3)$$

which is the Henderson–Hasselbalch equation [53]. For $pH = pK_c$ it is $N_c = N_n$ i.e. $[LF_{ox}H_2^+] = [LF_{ox}H]$.

The composition interplay of $LF_{ox}H$ and LF_{ox}^-, in aqueous solution for pH ≥ 7 is given by reaction (R2):

$$LF_{ox}H + OH^- \underset{k_{an}}{\overset{\kappa_{na}[OH^-]}{\rightleftharpoons}} LF_{ox}^- + H_2O. \quad (R2)$$

The steady-state ground-state equilibration dynamics between $LF_{ox}H$ and LF_{ox}^- is given by

$$\frac{dN_n}{dt} = k_{an}N_a - \kappa_{na}[OH^-]N_n = 0, \quad (4a)$$

$$\frac{dN_a}{dt} = -k_{an}N_a + \kappa_{na}[OH^-]N_n = 0, \quad (4b)$$

with

$$N_n + N_a = N_0, \quad (4c)$$

leading to

$$N_a = \frac{N_0}{1 + K_{a,OH}/[OH^-]} = \frac{N_0}{1 + 10^{-pK_{a,OH}}/10^{-pOH}} = \frac{N_0}{1 + 10^{pK_a - pK_w}/10^{pH - pK_w}} = \frac{N_0}{1 + 10^{pK_a}/10^{pH}}, \quad (4d)$$

with the anionic–neutral equilibrium constant $K_{a,OH} = k_{an}/\kappa_{na} = N_n[OH^-]/N_a$, $pK_{a,OH} + pK_a = pK_w$ and $pOH + pH = pK_w$. $K_w = [H^+][OH^-] \approx 10^{-14}\,(mol\,dm^{-3})^2$ is the ion product of water. N_a is the number density of anionic lumiflavin. $[OH^-]$ is the concentration of OH^-.

Solving Eq. (4a) for $[OH^-]$ gives $[OH^-] = (k_{an}/\kappa_{na})N_a/N_n = K_{a,OH}N_a/N_n$ or

$$pOH = -\log([OH^-]) = -\log(K_{a,OH}) - \log\left(\frac{N_a}{N_n}\right) = pK_{a,OH} - \log\left(\frac{N_a}{N_n}\right). \quad (5a)$$

With the relations $pOH = pK_w - pH$ and $pK_{a,OH} = pK_w - pK_a$ one obtains by insertion into Eq. (5a)

$$pH = pK_a + \log\left(\frac{N_a}{N_n}\right) = pK_a - \log\left(\frac{N_n}{N_a}\right). \quad (5b)$$

For $pH = pK_a$ it is $N_a = N_n$, i.e. $[LF_{ox}^-] = [LF_{ox}H]$.

The mole-fraction composition of $LF_{ox}H_2^+$ ($x_c = N_c/N_0$), $LF_{ox}H$ ($x_n = N_n/N_0$) and LF_{ox}^- ($x_a = N_a/N_0$) was determined by absorption measurements. The total absorption is the sum of the composite absorptions according to

$$\alpha(\lambda) = [x_c\sigma_c(\lambda) + x_n\sigma_n(\lambda) + x_a\sigma_a(\lambda)]N_0. \quad (6)$$

This relation was applied to Fig. 3a to extract x_c(pH), x_n(pH), and x_a(pH) shown in Fig. 3b. At pH −1.08 the still present fraction of neutral lumiflavin is found to be $x_n(pH\ -1.08) \approx 0.034$.

It should be noticed that Eqs. (2) and (3) are generally valid for the thermodynamic equilibrium between the cationic and neutral form of a molecular species in aqueous solution, and that Eqs. (4) and (5) are generally valid for the thermodynamic equilibrium between the neutral and the anionic form a molecular species in aqueous solution.

4.3. Excited-state dynamics

Information on the excited-state dynamics is obtained from fluorescence studies. The performed low-excitation-intensity fluorescence studies (spontaneous emission measurements) do not change the ground-state population distribution. The determined short excited state lifetimes of $LF_{ox}H^*$ ($\tau_{F,n} \approx 5.2$ ns for pH > 3), $LF_{ox}H_2^{+*}$ ($\tau_{F,c} \approx 0.4$ ps), and LF_{ox}^{-*} ($\tau_{F,a} \approx 90$ ps) hinder the formation of excited state equilibria between $LF_{ox}H^*$ and $LF_{ox}H_2^{+*}$ at low pH according to reaction R3, and between $LF_{ox}H^*$ and LF_{ox}^{-*} at high pH according to reaction (R4):

$$LF_{ox}H_2^{-*} + H_2O \underset{\kappa_{nc}^*[H^+]}{\overset{k_{cn}^*}{\rightleftharpoons}} LF_{ox}H^* + H_3O^+, \quad (R3)$$

$$LF_{ox}H^* + OH^- \underset{k_{an}^*}{\overset{\kappa_{na}^*[OH^-]}{\rightleftharpoons}} LF_{ox}^{-*} + H_2O. \quad (R4)$$

Since no excited-state equilibria are formed, the equilibrium constants $K_c^* = k_{cn}^*/\kappa_{nc}^*$ and $K_{a,OH}^* = k_{an}^*/\kappa_{na}^*$ or the corresponding values pK_c^* and $pK_a^* = pK_w - pK_{a,OH}^*$ are not accessible. One may define pK_{Fc}^* and pK_{Fa}^* values as the pH values where the fluorescence quantum yield is given by $\phi_F(pK_{Fc}^*) = (\phi_{F,c} + \phi_{F,n})/2$, and $\phi_F(pK_{Fa}^*) = (\phi_{F,n} + \phi_{F,a})/2$. The obtained values for lumiflavin are $pK_{Fc}^* \approx 1.8$ and $pK_{Fa}^* \approx 10.8$ ($\phi_{F,c} \approx \phi_F(pH\ -1.08, \lambda_{exc} = 400\,nm) \approx 3.6 \times 10^{-5}$, $\phi_{F,n} \approx \phi_F(pH\ 6) \approx 0.29$, $\phi_{F,a} \approx \phi_F(pH\ 14) \approx 0.0042$).

4.3.1. Low-pH excited-state dynamics

The excited-state dynamics of lumiflavin in the low pH range (pH < 7) is illustrated in Scheme 1. The cationic molecules $LF_{ox}H_2^+$ photo-excited to $LF_{ox}H_2^{+*}$ leave the excited state with the time constant $\tau_{F,c}$. The neutral molecules $LF_{ox}H$ photo-excited to $LF_{ox}H^*$ leave the excited state with the intrinsic time constant $\tau_{F,0,n}$ and convert to $LF_{ox}H_2^+$ by intermolecular protonation according to $LF_{ox}H^* + H^+ \rightarrow LF_{ox}H_2^+$. This rate of protonation is proportional to the H^+ concentration, and therefore grows exponentially with

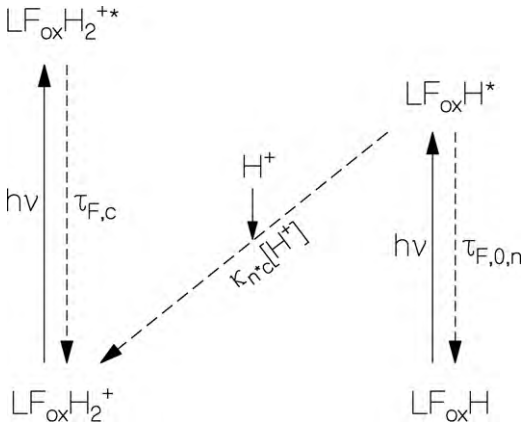

Scheme 1. Reaction dynamics of photo-excited lumiflavin at low pH (pH < 7).

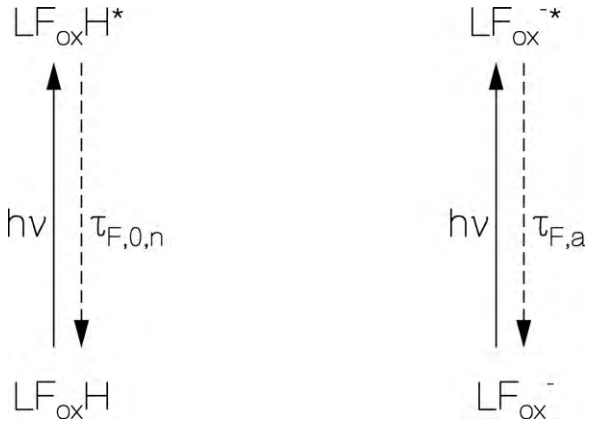

Scheme 2. Reaction dynamics of photo-excited lumiflavin at high pH (pH > 7).

decreasing pH. The excited-state dynamics according to Scheme 1 is given by

$$\frac{dN_n^*}{dt} = \frac{N_0 x_n I_{exc}(\lambda)\sigma_n(\lambda)}{h\nu_{exc}} - \frac{N_n^*}{\tau_{F,0,n}} - \kappa_{n^*c}[H^+]N_n^*, \tag{7a}$$

$$\frac{dN_c^*}{dt} = \frac{N_0 x_c I_{exc}(\lambda)\sigma_c(\lambda)}{h\nu_{exc}} - \frac{N_c^*}{\tau_{F,0,c}}. \tag{7b}$$

The first terms in Eqs. (7a) and (7b) give the excited state population by light absorption. The second terms in Eqs. (7a) and (7b) describe the intrinsic excited state depopulation. The third term in Eq. (7a) considers the conversion of $LF_{ox}H^*$ to $LF_{ox}H_2^+$ by intermolecular proton transfer according to $LF_{ox}H^* + H_3O^+ \rightarrow LF_{ox}H_2^+ + H_2O$.

The fluorescence decay constant of the neutral lumiflavin component is obtained from Eq. (7a) to be

$$\tau_{F,n} = \frac{1}{(1/\tau_{F,0,n}) + \kappa_{n^*c}[H^+]} = \frac{\tau_{F,0,n}}{1 + \kappa_{n^*c}[H^+]\tau_{F,0,n}}$$
$$= \frac{\tau_{F,0,n}}{1 + \tau_{F,0,n}\kappa_{n^*c}10^{-pH}\,\mathrm{mol\,dm^{-3}}}. \tag{8}$$

A fit to the experimental τ_F data is shown by the solid curve in Fig. 7a with a bi-molecular rate constant of $\kappa_{n^*c} = 1.2 \times 10^{10}\,\mathrm{mol^{-1}\,s^{-1}}$ and $\tau_{F,0,n} = 5.2$ ns. Analogously, the $LF_{ox}H$ fluorescence quantum yield is given by $\phi_{F,n} = \tau_{F,n}/\tau_{rad,n}$, leading to

$$\phi_{F,n} = \frac{\tau_{F,n}}{\tau_{rad,n}} = \frac{\phi_{F,0,n}}{1 + \tau_{F,0,n}\kappa_{n^*c}10^{-pH}\,\mathrm{mol\,dm^{-3}}}. \tag{9}$$

Eq. (9) has the same form as Eq. (8). $\phi_{F,0,n} = \tau_{F,0,n}/\tau_{rad,n}$ is the intrinsic fluorescence quantum yield of the neutral form of lumiflavin (situation of negligible excited-state neutral form deactivation by intermolecular proton transfer as it is the case around pH 6). The fit curve with $\phi_{F,0,n} = 0.29$, $\kappa_{n^*c} = 1.2 \times 10^{10}\,\mathrm{mol^{-1}\,s^{-1}}$ and $\tau_{F,0,n} = 5.2$ ns is shown by the solid curve in Fig. 5.

The fluorescence lifetime of $LF_{ox}H$ at pH −1.08 (fraction of neutral molecules there is $x_n = 0.034$) is calculated from Eq. (8) to be $\tau_{F,n}(pH\,-1.08) = 6.8$ ps.

4.3.2. High-pH excited-state dynamics

The excited-state dynamics of the neutral and anionic forms of lumiflavin in the high-pH range (pH > 7) is effectively uncoupled (the intermolecular protonation of $LF_{ox}{}^{-*}$ according to $LF_{ox}{}^{-*} + H^+ \rightarrow LF_{ox}H$ is negligible at high pH because of negligible H^+ concentration). The decoupled photo-excitation scheme for $LF_{ox}H$ and $LF_{ox}{}^-$ is shown in Scheme 2. The excited state relaxation dynamics according to Scheme 2 is given by

$$\frac{dN_n^*}{dt} = \frac{N_0 x_n I_{exc}(\lambda)\sigma_n(\lambda)}{h\nu_{exc}} - \frac{N_n^*}{\tau_{F,0,n}}, \tag{10a}$$

$$\frac{dN_a^*}{dt} = \frac{N_0 x_a I_{exc}(\lambda)\sigma_a(\lambda)}{h\nu_{exc}} - \frac{N_a^*}{\tau_{F,a}}. \tag{10b}$$

After excitation the fluorescence signal is given by

$$S_F(t) = \kappa'\left[\frac{N_{n,0}^*}{\tau_{rad,n}}\exp\left(-\frac{t}{\tau_{F,0,n}}\right) + \frac{N_{a,0}^*}{\tau_{rad,a}}\exp\left(-\frac{t}{\tau_{F,a}}\right)\right]$$
$$= \kappa'\left[\frac{x_n(pH)\sigma_n(\lambda_{exc})}{\tau_{rad,n}}\exp\left(-\frac{t}{\tau_{F,0,n}}\right) + \frac{x_a(pH)\sigma_a(\lambda_{exc})}{\tau_{rad,a}}\exp\left(-\frac{t}{\tau_{F,a}}\right)\right]. \tag{11}$$

For the second equality the proportionalities $N_{n,0}^* = \mathrm{const} \times x_n(pH)\sigma_n(\lambda_{exc})N_0$ and $N_{a,0}^* = \mathrm{const} \times x_a(pH)\sigma_a(\lambda_{exc})N_0$ are used.

The fraction of the long-time fluorescence signal initial height, $x_{F,n}$, due to neutral excited state emission is

$$x_{F,n}(pH) = \frac{x_n(pH)\sigma_n(\lambda_{exc})/\tau_{rad,n}}{(x_n(pH)\sigma_n(\lambda_{exc})/\tau_{rad,n}) + (x_a(pH)\sigma_a(\lambda_{exc})/\tau_{rad,a})}$$
$$= \frac{1}{1 + (\tau_{rad,n}/\tau_{rad,a})(x_a(pH)\sigma_a(\lambda_{exc})/x_n(pH)\sigma_n(\lambda_{exc}))}, \tag{12a}$$

whereby $x_a(pH) = 1 - x_n(pH)$. The fraction of the short-time fluorescence signal initial height, $x_{F,a}$, due to anionic excited state emission is

$$x_{F,a}(pH) = 1 - x_{F,n}(pH). \tag{12b}$$

The curves $x_{F,n}$ and $x_{F,a}$ are displayed in Fig. 7b.

4.4. Intrinsic fluorescence behaviour of neutral, cationic and anionic lumiflavin

The fluorescence behaviour of neutral flavin dissolved in aqueous solution in the range pH > 3 is determined by photo-physical relaxation (internal conversion and intersystem crossing). The S_1-state potential energy surface is determined by vibronic relaxation and solvatation due to excited-state dipole moment changes [54–58] (adiabatic optical electron transfer [47,59]). A potential energy curve illustration is shown in the middle position of the lower row of Fig. 1 (potential curves are called spectroscopic states according to [60], relaxation in S_1 potential energy surface from the locally excited state position LE to vibrational and solvatation relaxed position SR). The structural formulae of $LF_{ox}H$ (upper row of Fig. 1) and of $LF_{ox}H^*$ (middle row of Fig. 1) are the same. The rather large Stokes shift, $\delta\tilde{\nu}_{St} = \lambda_{a,max}^{-1} - \lambda_{F,max}^{-1}$, between absorption and emission maxima and the rather broad S_0–S_1 absorption ($\Delta\tilde{\nu}_a$) and S_1–S_0 emission ($\Delta\tilde{\nu}_{em}$) bandwidths (FWHM), listed in Table 1, are due to the solvatation dynamics.

The fluorescence behaviour of cationic flavin present at low pH (dominant for pH < $pK_c = 0.38$) is thought to be determined

by barrier-less intra-molecular charge transfer between locally excited state (LT) and charge transfer state (CT) (diabatic electron transfer [47,59]). A potential energy curve illustration is shown at the lower left part of Fig. 1 (a surface touching state situation [60] is sketched, but barrier-less conical intersection cannot be excluded). A possible structural formula of $LF_{ox}H_2^{+*}$ is shown at the left part of the middle row of Fig. 1 (positive charge movement from N10 to N1, other charge movement cannot be excluded, computational chemical calculations would be necessary for clarification). The extremely small fluorescence quantum yield and the very short fluorescence lifetime indicate a practically barrier-less S_1 state potential energy surface along the reaction coordinate [60] to surface touching with the S_0 ground state or conical intersection with the S_0 ground state.

The fluorescence behaviour of anionic lumiflavin present at high pH (dominant for $pH > pK_a = 10.8$) is also thought to determined by intra-molecular charge transfer (diabatic electron transfer [47,59]) from locally excited state (LT) to charge transfer state (CT). A possible potential energy curve illustration is shown at the lower right part of Fig. 1 (a sloped conical intersection situation [59] is sketched). A possible structural formula of LF_{ox}^{-*} is shown at the right part of the middle row of Fig. 1 (negative charge movement from N3 to O2, also possible may be charge movement from N3 to O4, quantum chemical calculations might clarify the potential energy surface structure and charge distribution). The moderate fluorescence quantum yield ($\phi_{F,a} \approx 0.0042$) and moderate fluorescence lifetime ($\tau_{F,a} \approx 90$ ps) of LF_{ox}^- indicate a potential barrier before conical intersection between the excited-state potential energy surface and the ground-state energy surface as indicated in the potential energy surface scheme (lower right part of Fig. 1).

4.5. Comparison with other flavins

The pH dependent absorption and emission of lumiflavin behaves similar to the pH dependent absorption and emission of other flavins where the methyl group at N10 is replaced with another group [1,2,41]. Relative fluorescence quantum yields versus pH are given in [26,27] for riboflavin and lumiflavin. Absorption cross-section spectra, fluorescence quantum distributions, and fluorescence decay curves for riboflavin in aqueous solutions in the pH range from −1.1 to 13.4 are shown in [45]. The findings in [45] on riboflavin are similar to the findings here on lumiflavin (blue-shifted absorption spectrum at low pH, vanishing fluorescence at low pH, low fluorescence at high pH, bi-exponential fluorescence decay at high pH). The reported pK and pK_F^* values for lumiflavin, riboflavin and FMN are collected in Table 2. For all three cases around pH 0 (pK_c) the concentrations of cationic and neutral form are equal, and around pH 10 (pK_a) the concentrations of neutral and anionic form are equal [1,2,41,49]. For lumiflavin and riboflavin (no data found for FMN) the fluorescence quantum yield reduces to half of its neutral pH value at $pH \approx 2$ (pK_{Fc}^*) and to the mid-point value between neutral and anionic form at $pH \approx 10$ (pK_{Fa}^*). In both cases it is $pK_{Fc}^* > pK_c$ (fluorescence quenching of neutral excited flavin due to external proton transfer) and $pK_{Fa}^* = pK_a$ (no external proton transfer at high pH).

5. Conclusions

The absorption and emission behaviour of lumiflavin in the flavoquinone redox state in aqueous solution was studied over a pH range from −1.08 to 14.6. For $pH < pK_c = 0.38$ lumiflavin is dominantly present in cationic form. The cationic lumiflavin has an alloxazine-like double-bond electron structure and an alloxazine-like absorption spectrum. Its fluorescence is strongly quenched likely by barrier-less intra-molecular charge transfer and excited state relaxation likely by potential surface touching or conical intersection with the ground state.

In the range $0.38 = pK_c < pH < pK_a = 10.8$ lumiflavin is dominantly present in neutral form. It has the typical isoalloxazine double-bond electron structure and isoalloxazine-like absorption spectrum. The intrinsic fluorescence behaviour is determined by solvatation dynamics and photo-physical relaxation (internal conversion and intersystem crossing). The fluorescence efficiency above pH 3 is rather high. In the low pH range (<pH 3) the neutral lumiflavin fluorescence quantum yield is reduced and the fluorescence lifetime is shortened by excited-state hydronium-ion (H_3O^+) mediated conversion of neutral lumiflavin to cationic lumiflavin (intermolecular photo-induced proton transfer according to $LF_{ox}H^* + H_3O^+ \rightarrow LF_{ox}H_2^+ + H_2O$).

In the range $pH > pK_a = 10.8$ lumiflavin is dominantly present in anionic form. It remains the typical isoalloxazine double-bond electron structure and isoalloxazine-like absorption spectrum. The fluorescence of anionic lumiflavin is quenched likely by intra-molecular charge transfer and excited state relaxation via a sloped conical intersection. The pH dependent fluorescence behaviour coincides with the pH dependent absorption behaviour ($pK_a = pK_{Fa}^*$) (intermolecular protonation, $LF_{ox}^{-*} + H^+ \rightarrow LF_{ox}H$, cannot occur because of lack of H^+ concentration at high pH).

Acknowledgements

The authors thank the Deutsche Forschungsgemeinschaft (DFG) for support in the Graduate College GK 640 “Sensory photoreceptors in natural and artificial systems” and in the Research Group FOR 526 “Sensory Blue Light Receptors”. A.P. is grateful to Profs. F.J. Gießibl and J. Repp for their kind hospitality.

References

[1] F.P. Heelis, The photophysical and photochemical properties of flavins (isoalloxazines), Chem. Soc. Rev. 11 (1982) 15–39.
[2] F. Müller (Ed.), Chemistry and Biochemistry of Flavoenzymes, vol. 1, CRC Press, Boca Raton, FL, 1991.
[3] J. Kozoil, Studies on flavins in organic solvents—III. Spectral behaviour of lumiflavin, Photochem. Photobiol. 9 (1969) 45–53.
[4] J. Koziol, E. Knobloch, The solvent effect on the fluorescence and light absorption of riboflavin and lumiflavin, Biochim. Biophys. Acta 102 (1965) 289–300.
[5] M. Green, G. Tollin, Flash photolysis of flavins. I. Photoreduction in non-aqueous solvents, Photochem. Photobiol. 7 (1968) 129–143.
[6] P.-S. Song, D.E. Metzler, Photochemical degradation of flavins—IV. Studies of the anaerobic photolysis of riboflavin, Photochem. Photobiol. 6 (1967) 691–709.
[7] I. Ahmad, S. Ahmed, M.A. Sheraz, F.H.M. Vaid, Effect of borate buffer on the photolysis of riboflavin in aqueous solution, J. Photochem. Photobiol. B 93 (2008) 82–87.
[8] P. Hemmerich, S. Fallab, H. Erlenmeyer, Synthesen in der Lumiflavinreihe, Helv. Chim. Acta 39 (1956) 1242–1252.
[9] P. Byrom, J.H. Turnbull, Excited states of flavine coenzymes—II. Anaerobic oxidation of amino acids by excited riboflavine devrivatives, Photochem. Photobiol. 6 (1967) 125–131.
[10] F. Müller, A two-step chemical synthesis of lumiflavin, Methods Enzymol. 66 (1980) 265–267.
[11] E. Choe, R. Huang, D.B. Min, Chemical reactions and stability of riboflavin in foods, J. Food Sci. 70 (2005) R28–R36.
[12] M.S. Grodowski, B. Veyret, K. Weiss, Photochemistry of flavins. II. Photophysical properties of alloxazines and isoalloxazines, Photochem. Photobiol. 26 (1977) 341–352.
[13] A. Yoshimura, T. Ohno, Lumiflavin-sensitized photooxygenation of indole, Photochem. Photobiol. 48 (1988) 561–565.
[14] M.Y. Jung, D.B. Min, ESR study of singlet oxygen quenching and protective activity of trolox on the photodecomposition of riboflavin and lumiflavin in aqueous buffer solutions, J. Food Sci. 74 (2009) C449–C455.
[15] A. Knowles, E.M.F. Roe, A flash-photolysis investigation of flavin photosesitization of purine nucleotides, Photochem. Photobiol. 7 (1968) 421–436.
[16] C.H. Suelter, D.R. Metzler, The oxidation of a reduced pyridine nucleotide analog by flavins, Biochim. Biophys. Acta 44 (1960) 23–33.
[17] R. Huang, H.J. Kim, D.B. Min, Photosensitizing effect of riboflavin, lumiflavin, and lumichrome on the generation of volatiles in soy milk, J. Agric. Food Chem. 54 (2006) 2359–2364.
[18] J. Koziol, Absorption spectra of riboflavin, lumiflavin, and lumichrome in organic solvents, Experientia 21 (1965) 189–190.

[19] A Bowd, P. Byrom, J.B. Hudson, J.H. Turnbull, Excited states of flavine coenzymes—III. Fluorescence and phosphorescence emissions, Photochem. Photobiol. 8 (1968) 1–10.
[20] M. Sun, T.A. Moore, P.-S. Song, Molecular luminescence studies of flavins. I. The excited states of flavins, J. Am. Chem. Soc. 94 (1972) 1730–1740.
[21] S.P. Vaish, G. Tollin, Flash photolysis of flavins. IV. Some properties of the lumiflavin triplet state, J. Bioenerg. 1 (1970) 181–192.
[22] N. Lasser, J. Feitelson, Excited-state reactions of oxidized flavin derivatives, Photochem. Photobiol. 21 (1975) 249–254.
[23] E. Sikorska, I.V. Khmelinskii, J. Koput, M. Sikorski, Electronic structure of lumiflavin and its analogues in their ground and exited states, Theochem 676 (2004) 155–165.
[24] A. Penzkofer, A.K. Bansal, S.-H. Song, B. Dick, Fluorescence quenching of flavins by reductive agents, Chem. Phys. 336 (2007) 14–21.
[25] W. Holzer, J. Shirdel, P. Zirak, A. Penzkofer, P. Hegemann, R. Deutzmann, E. Hochmuth, Photo-induced degradation of some flavins in aqueous solution, Chem. Phys. 308 (2005) 69–78.
[26] F. Kavanagh, R.H. Goodwin, The relationship between pH and fluorescence of several organic compounds, Arch. Biochem. 20 (1949) 315–324.
[27] R. Kuhn, G. Moruzzi, Über die Dissoziationskonstanten der Flavine; p_H-Abhängigkeit der Fluoreszenz, Ber. Deut. Chem. Ges. 67 (1934) 888–891.
[28] S.G. Schulman, pH dependence of fluorescence of riboflavin and related isoalloxazine derivatives, J. Pharm. Sci. 60 (1971) 628–631.
[29] L. Michaelis, M.P. Schubert, C.V. Smythe, Potentiometric study of flavins, J. Biol. Chem. 116 (1936) 587–607.
[30] S. Schreiner, U. Steiner, H.E.A. Kramer, Determination of the p*K* values of the lumiflavin triplet state by flash photolysis, Photochem. Photobiol. 21 (1975) 81–84.
[31] A.R. Surrey, F.C. Nachod, Alkaline hydrolysis of riboflavin, J. Am. Chem. Soc. 73 (1951) 2236–2238.
[32] R. Kuhn, H. Rudy, Über den alkalilabilen Ring des Lacto-flavins, Ber. Deut. Chem. Ges. 67 (1934) 892–898.
[33] C.B. Martin, X. Shi, M.-L. Tsao, D. Karweik, J. Brooke, C.M. Hadad, M.S. Platz, The photochemistry of riboflavin tetraacetate and nucleosides. A study using density functional theory, laser flash photolysis, fluorescence, UV–Vis and time resolved infrared spectroscopy, J. Phys. Chem. 106 (2002) 10263–10271.
[34] M. Takahashi, Y. Ishikawa, J. Nishizawa, H. Ito, Low-frequency vibrational modes of riboflavin and related compounds, Chem. Phys. Lett. 401 (2005) 475–482.
[35] M. Kondo, J. Nappa, K.L. Ronayne, A.L. Stelling, P.J. Tonge, S.R. Meech, Ultrafast vibrational spectroscopy of the flavin chromophore, J. Phys. Chem. B 110 (2006) 20107–20271.
[36] M.M.N. Wolf, C. Schumann, R. Gross, T. Domratcheva, R. Diller, Ultrafast infrared spectroscopy of riboflavin: dynamics, electronic structure, and vibrational mode analysis, J. Phys. Chem. B 112 (2008) 13424–13432.
[37] S. Salzmann, C.M. Marian, Effects of protonation and deprotonation on the excitation energies of lumiflavin, Chem. Phys. Lett. 464 (2008) 400–404.
[38] S. Salzmann, J. Tatchen, C.M. Marian, The photophysics of flavins: what makes the difference between gas phase and aqueous solution? J. Photochem. Photobiol. A 198 (2008) 221–231.
[39] J. Hasegawa, S. Bureekaew, H. Nakatsuji, SAC-CI theoretical study on the excited states of lumiflavin: structure, excitation spectrum and solvation effect, J. Photochem. Photobiol. A 189 (2007) 205–210.
[40] K. Zenichowski, M. Gothe, P. Saalfrank, Exciting flavins: absorption spectra and spin-orbit coupling in light-oxygen-voltage (LOV) domains, J. Photochem. Photobiol. A 190 (2007) 290–300.
[41] F. Müller, S. Ghisla, A. Bacher, 2. Vitamin B_2 und natürliche Flavine, in: O. Isler, G. Brubacher, S. Ghisla, K. Kräutler (Eds.), Vitamine II, Thieme Verlag, Stuttgart, 1988, pp. 50–159.
[42] Y.-T. Kao, C. Saxena, T.-F. He, L. Guo, L. Wang, A. Sancar, D. Zhong, Ultrafast dynamics of flavins in five redox states, J. Am. Chem. Soc. 130 (2008) 13132–13139.
[43] S.-H. Song, B. Dick, A. Penzkofer, Photo-induced reduction of flavin mononucleotide in aqueous solutions, Chem. Phys. 332 (2007) 55–65.
[44] S.-H. Song, B. Dick, A. Penzkofer, P. Hegemann, Photo-reduction of flavin mononucleotide to semiquinone form in LOV domain mutants of blue-light receptor phot from *Chlamydomonas reinhardtii*, J. Photochem. Photobiol. B: Biol. 87 (2007) 37–48.
[45] P. Drössler, W. Holzer, A. Penzkofer, pH dependence of the absorption and emission behaviour of riboflavin in aqueous solution, Chem. Phys. 282 (2002) 429–439.
[46] M. Mardelli, J. Olmsted III, Calorimetric determination of the 9,10-diphenylanthracene fluorescence quantum yield, J. Photochem. 7 (1977) 277–285.
[47] P. Zirak, A. Penzkofer, T. Mathes, P. Hegemann, Photo-dynamics of roseoflavin and riboflavin in aqueous and organic solvents, Chem. Phys. 358 (2009) 111–122.
[48] B. Meier, A. Penzkofer, Picosecond pulse generation in a benzene Raman generator amplifier system, Appl. Phys. B 53 (1991) 65–70.
[49] K.H. Dudley, A. Ehrenberg, P. Hemmerich, F. Müller, Spektren und Strukturen der am Flavin-Redoxsystem beteiligten Partikeln, Helv. Chim. Acta 47 (1964) 1354–1383.
[50] S.J. Strickler, R.A. Berg, Relationship between absorption intensity and fluorescence lifetime of molecules, J. Chem. Phys. 37 (1962) 814–822.
[51] J.B. Birks, D.J. Dyson, The relations between the fluorescence and absorption properties of organic molecules, Proc. Roy. Soc. London Ser. A 275 (1963) 135–148.
[52] A.V. Deshpande, A. Beidoun, A. Penzkofer, G. Wagenblast, Absorption and emission spectroscopic investigation of cyanovinyldiethylaniline dye vapors, Chem. Phys. 142 (1990) 123–131.
[53] R. de Levie, The Henderson approximation and the mass action law of Guldberg and Waage, Chem. Educ. 7 (2002) 132–135.
[54] C. Reichardt, Solvents and Solvent Effects in Organic Chemistry, VCH, Weinheim, 1988.
[55] M. Mataga, T. Kubota, Molecular Interaction and Electronic Spectra, Dekker, New York, 1970.
[56] M.L. Horng, J.A. Gardecki, A. Papazyan, M. Maroncelli, Subpicosecond measurements of polar solvation dynamics: coumarin 153 revisited, J. Phys. Chem. 99 (1995) 17311–17337.
[57] J.D. Simon, Solvation dynamics: new insights into chemical reaction and relaxation processes, Pure Appl. Chem. 62 (1990) 2243–2250.
[58] G.R. Fleming, Chemical Applications of Ultrafast Spectroscopy, Oxford University Press, New York, 1986.
[59] K.-Y. Chen, C.-C. Hsieh, Y.-M. Cheng, C.-H. Lai, P.-T. Chou, T.J. Chow, Tuning excited-state electron transfer from an adiabatic to nonadiabatic type in donor–bridge–acceptor systems and the associated energy-transfer process, J. Phys. Chem. A 110 (2006) 12136–12144.
[60] N.J. Turro, V. Ramamurthy, H.C. Scaiano, Principles of Molecular Photochemistry. An Introduction, University Science Books, Sausalito, CA, 2009.
[61] A. Albert, Quantitative studies of the avidity of naturally occurring substances for trace metals. 3. Pteridines, riboflavin and purines, Biochem. J. 54 (1953) 646–654.